Simultaneous Context Inference and Mapping using mm-Wave for Indoor Scenarios

Ali Yassin,Youssef Nasser,Mariette Awad, Ahmed Al-Dubai++
ECE Department, Faculty of Engineering and Architecture, American University of Beirut, Lebanon
++School of Computing, Edinburgh Napier University, UK

***Abstract*—We introduce in this paper two main approaches, Triangulateration (TL) and Angle-Difference-of-Arrival (ADoA) for indoor localization and mapping using single-anchor and millimeter wave (MMW) propagation characteristics. Then, we perform context inference through obstacle localization. To do so, we first include and estimate the positions of virtual anchor nodes (VANs), known as mirrors of the real anchor with respect to obstacle. Then, it is followed by estimating the obstacle position and its dimensions. We assess the performance of each technique via cumulative distribution function (CDF) for the location estimation root mean square error (RMSE). Simulations confirm that localization of the receiver relying on a single anchor and the localization of obstacles in MMW achieves a few centimeters accuracy.**

***Index Terms*—Millimeter wave, Triangulateration (TL), Angle-Difference-of-Arrival (ADoA), virtual anchor node (VAN), obstacle detection.**

I. Introduction

MilliMeter Wave (MMW) wireless communication systems have recently gained great research interests due to their benefits in terms of spectrum, propagation characteristics, potential applications and services [1][2]. Applications based on multi gigabit data rates are increasing in demands. Hence, MMW is evolving due to the availability of a large bandwidth. Basically, MMW spectrum ranges between 30 GHz and 300 GHz. Technically, MMW spectrum can be used for military, radar and cellular services. For instance, the spectrum at 28 GHz, 38 GHz, and 70-80 GHz provides promising channel propagation specifications for the evolving fifth generation (5G) of cellular systems [3][4]. The indoor networking of 5G mobile wireless communication is based on 60 GHz technology that is embracing the "small cell" deployment. The fact that 60 GHz signals are of short-range nature because of high atmospheric absorption and high path loss makes them suitable for implementing this technique due to the reduction of self-interference. Moreover, the shortness of the coverage range of access points operating at millimeter wave frequencies triggers the deployment of a capillary network of access points in the buildings offering enhancements in terms of localization. Among the potential services offered by MMW, localization and mapping appears as key factor in enabling new means and tools for communications systems [5]. Moreover, Indoor Positioning Systems (IPSs) are the center of attention for researchers because of the vast technological enhancement in smartphones and tablets, and the evolving technology of Internet of Things (IoT) as a future service in 5G. For instance, localization is critical for detecting products stored in a warehouse, medical equipment and personnel in a hospital, firemen in a building with fire, etc. With the evolution of MMW communication systems, IPSs will exploit the infrastructure of future MMW groundwork. In terms of channel propagation, research works showed that MMW channel behaves as the quasi-optical channel; hence, the Line of Sight (LoS) factor is dominant [6]. Thus, MMW channel models take into account only double-bounce reflection effect since higher order of bounces for non-Line of Sight (NLoS) paths is deteriorated at mm-wave frequencies [7]. The characteristics of the channel at those frequencies showed that reflections do not generate significant amount of scattering [8], and that the transmitted beam will have the same directivity after reflections with slight scattering [9]. Hence, Snells law holds in terms of the equality between the angles of departure and incidence upon reflection [10]. These propagation characteristics could be then used for localization and mapping. However, localization procedures and mapping approaches should be derived to have appropriate channel models[4][11][12]. In the literature, there exist few researches on localization systems operating at 60 GHz. Most of the research work done focused on measuring the delay spread used for systems based on Time-of-Arrival (TOA), Time-Difference-of-Arrival (TDOA) and Angle-of-Arrival (AoA) methods [13][14]. For instance, the proposed method in [15] extracts the TDoA from the interferences between the OFDM signals transmitted by two antennas at 60 GHz. Moreover, received signal strength indicator (RSSI) localization systems have been used mainly at WiFi, WiMax and UWB bands [16] [17]. In this paper, the proposed localization techniques allow us to develop context inference and mapping of the indoor environment. As well, they achieve very high accuracy reaching sub-meters (few centimeters in some cases). Hence, they could be easily adopted for IoT applications mainly in health, fire and emergency. In conclusion, our contribution can be summarized in the following aspects:

- We use the concept of Virtual Anchor Nodes (VANs) to estimate the location of the receiver through a single anchor node using the proposed Triangulateration (TL) technique and Angle-Difference-of-Arrival(ADoA)[18].
- We estimate the positions of VANs by moving the receiver into another known positions using TL.
- We provide detection of horizontal and vertical obstacles in the presence of a single transmitter

The rest of this paper is organized as follows. In Section 2, we develop the system model and the localization methodology of the receiver using MMW. In Section 3, we propose new approaches for context inference by estimating obstacles positions and dimensions. In Section 4, we provide simulation results while conclusions are drawn in Section 5.

II. System Model using Millimeter Wave

The proposed MMW localization technique are tested in an indoor environment consisting of a rectangular room

978-1-4673-8999-0/17/$31.00 ©2017 IEEE

bounded by four walls, the ceiling and the floor. The room boundaries and radio-reflective obstacles in the reflective objects are grouped in a set O. Obstacles are described as two-dimensional flat polygonal faces with sharp vertices and straight edges. Each oriented surface S is denoted by its perpendicular line, written as:

$$y = p_y + \alpha * (x - p_x) \tag{1}$$

where $\mathbf{p} = \left(p_x, p_y\right)$ is a point of intersection between the surface and its perpendicular line, and α is the slope of the line orthogonal to the surface S. By assumption, a single MMW Access Point (AP) is deployed in the room at a location $\mathbf{p}_{Tx}$. Additionally, the AP is assumed to broadcast its position and the specifications of the objects in O to the node(s) targeted for localization. This assumption holds for devices used for localization with hard energy limitations. The AoA spectrum, $P_p(\theta)$, is a $2 \times N_p$ matrix that records the amplitude of each multi path component (MPC) as a function of the azimuth θ at a given location $\mathbf{p}$, where N_p is the number of MPCs. Each MPC can be either due to a LOS link between the transmitter and the receiver or due to NLOS link caused by reflections of one or more surfaces in the obstacle set O. Then, $SP_p(\theta)$ is a $2 \times N_p$ matrix, which contains in its first row the amplitude of each MPC sorted in decreasing order and in its second row the azimuth θ with respect to reference angle θ_0. Hence, each column of $SP_p(\theta)$ is seen as a vector of polar coordinates that represents the amplitude and the phase of the vector relative to θ_0. Moreover, the room geometry is assumed to be known for user(s) to be localized.

A. Virtual Anchors

The first column vector of $SP_p(\theta)$ represents the LOS path between the transmitter and the receiver to be localized, and the columns $2 : N_p$ represent the NLOS paths. Thus, we have $N_p - 1$ MPCs that correspond to NLOS paths. Each of these paths can be modeled as emitted by a virtual anchor node through a virtual LOS path reaching the receiver $\mathbf{p}$. The locations of the virtual anchor nodes are determined by mirroring the AP $\mathbf{p}_{Tx}$ with respect to the surfaces in the obstacle set O since it is the source of signal reflections. We denote $VA = \{va_0, va_1, \ldots\}$ to be the set of the positions of all possible virtual anchor nodes, and we denote $\overline{VA} = \{VA_0, VA_1, \ldots\}$ to a partition of VA. We let $VA_0 = \mathbf{p}_{Tx}$, and each set $VA_i, i = 1, 2, \ldots$ represents all virtual anchor nodes that has been mirrored i times due to reflections caused by any surface in the obstacle set O. Actually, there is no limit on the number of reflections of the signal transmitted by $\mathbf{p}_{Tx}$. However, a MMW signal fades quickly during its propagation as it reflects off the surfaces. So, we limited the set VA by assuming a maximum reflection order μ[19]. So, the set of all VANs will be represented as $VA_\mu = \bigcup_{i=0}^{\mu} VA_i$. As shown in Figure 1, the anchors va_i and va_j represent first and second order of reflection respectively; hence, $va_i \in A_1$ and $va_j \in A_2$.

B. Localization Approaches

1) The Triangulateration (TL) Algorithm: This algorithm is based on estimating the location of an unknown receiver of position $\mathbf{p}$ using a set of triangulation steps followed by a verification of the estimated positions. It would be easier to estimate the position of the receiver through a direct triangulation method if we know the association between the virtual anchor nodes in VA and the MPCs in $SP_p(\theta)$. However, this association is unknown; hence, we have to estimate the position via set of triangulateration steps that are shown to be less complex than the method of maximum-likelihood (ML)[20]. Moreover, we restrict the set VA to reach a maximum reflection order μ_{max}. Actually, a low value of makes more sense for triangulateration since reflections fade the signal; thus, virtual anchor nodes of high reflection order can be far away from the receiver. TL steps are based on

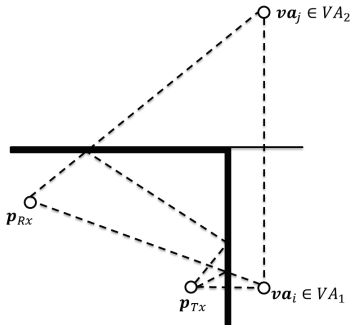

Fig. 1. VANs related to first and second order of reflections

forming a triangle between the unknown receiver and each anchor node. As shown in Figure 2, we can construct the following relations using trigonometric relations in the right triangle formed as follows:

$$x_{va_i} - x_{Rx} = \rho_i * \cos\theta_i \tag{2}$$

$$y_{va_i} - y_{Rx} = \rho_i * \sin\theta_i \tag{3}$$

where $\mathbf{va}_i = (x_{va_i}, y_{va_i})$ and $\mathbf{p}_{Rx} = (x_{Rx}, y_{Rx})$ are the virtual anchor node and the unknown receiver respectively. Also, θ_i and ρ_i are the AoA and the distance of the MPC transmitted virtually from the virtual anchor node $\mathbf{va}_i$ to the receiver at position $\mathbf{p}_{Rx}$, respectively. Then for each pair of virtual anchor

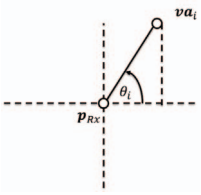

Fig. 2. Triangle formed between $\mathbf{va}_i$ and $\mathbf{p}_{Rx}$

nodes $\mathbf{va}_i$ and $\mathbf{va}_j$, we solve the system of equations in (2) and (3) corresponding to $\mathbf{va}_i$ with those corresponding to $\mathbf{va}_j$ to obtain the following system of equations:

$$x_{va_i} - x_{va_j} = \rho_i * \cos\theta_i - \rho_j * \cos\theta_j \tag{4}$$

$$y_{va_i} - y_{va_j} = \rho_i * \sin\theta_i - \rho_j * \sin\theta_j \tag{5}$$

The above system of equation can be written using matrix notation as follows:

$$\mathbf{VA}_{i,j} = \mathbf{\Gamma} * \mathbf{P} \tag{6}$$

where $\mathbf{VA}_{i,j}$,$\mathbf{\Gamma}$, and $\mathbf{P}$ are defined as follows:

$$\mathbf{VA}_{i,j} = \begin{bmatrix} x_{va_i} - x_{va_j} \\ y_{va_i} - y_{va_j} \end{bmatrix}$$

$$\mathbf{\Gamma} = \begin{bmatrix} \cos\theta_i & -\cos\theta_j \\ \sin\theta_i & -\sin\theta_j \end{bmatrix}$$

$$\mathbf{P} = \begin{bmatrix} \rho_i \\ \rho_j \end{bmatrix}$$

Solving (6), we obtain the following:

$$\mathbf{P} = \mathbf{\Gamma}^{-1} * \mathbf{VA}_{i,j} \tag{7}$$

After solving for $\mathbf{P}$, the estimation of the position $\mathbf{p}_{Rx}$ of the receiver can be done by replacing ρ_i in (4) and (5). The TL steps are repeated for all possible pairs of $(\mathbf{va}_i, \mathbf{va}_j), i \neq j$ in the set VA_{max}. So, we will obtain K estimates of the receiver position. The final estimate will be the average of all estimates $\mathbf{p}_k, k = 1, 2, \ldots K$.

C. The Angle Differences-of-Arrival (ADoA) Technique

The TL method is based on the azimuth θ of all MPCs with respect to reference angle θ_0. The knowledge of θ_0 is assumed to be known; however, this may not be a valid assumption due to the error in the measurement of θ_0 that may be done using a digital compass of a smartphone. Hence, this shed the light on a second technique based on the Angle Differences-of-Arrival (ADoA) among MPCs. ADoA doesnt require the knowledge of θ_0 since it will be neglected in the difference between two AoA values. In ADoA, we take all possible triplets of VANs $(\mathbf{va}_i, \mathbf{va}_j, \mathbf{va}_q), i \neq j \neq q$, and we define the angle of differences as follows:

$$\delta_1 = SP_{p2,j} - SP_{p2,i} \tag{8}$$

$$\delta_2 = SP_{p2,q} - SP_{p2,j} \tag{9}$$

As shown in Figure 3, the trajectory of receiver $\mathbf{p}_{Rx}$ is a circle

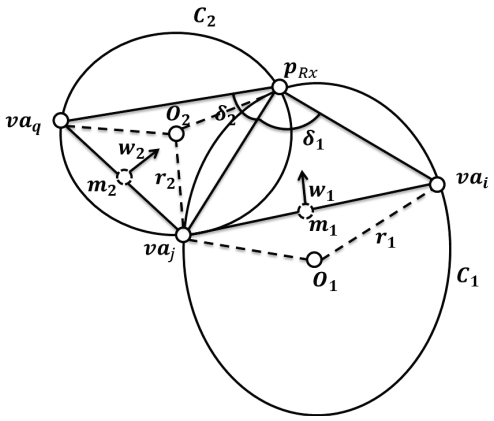

Fig. 3. The geometry of ADoA localization Technique

where $\mathbf{va}_i\widehat{\mathbf{p}_{Rx}}\mathbf{va}_j$ is constant and equals to δ_1. As well, we assume $\mathbf{va}_i\widehat{\mathbf{p}_{Rx}}\mathbf{va}_j > 0$ if $\mathbf{va}_i$ follows $\mathbf{va}_j$ in a counterclockwise direction within the semi-circle and $\left|\mathbf{va}_i\widehat{\mathbf{p}_{Rx}}\mathbf{va}_j\right| < \pi$, where |.| operator generates the absolute value of the measured angle. Consider the circumference C_1 in Figure 3; we use the relation between central and vertex angles intercepting the same chord $(\overline{\mathbf{va}_i\mathbf{va}_j})$ in a circle to obtain the following relation:

$$\mathbf{va}_i\widehat{\mathbf{o}_1}\mathbf{va}_j = 2 * \mathbf{va}_i\widehat{\mathbf{p}_{Rx}}\mathbf{va}_j = 2 * \delta_1 \tag{10}$$

If $\mathbf{va}_i\widehat{\mathbf{p}_{Rx}}\mathbf{va}_j > \pi/2$, then $\left|\mathbf{va}_i\widehat{\mathbf{o}_1}\mathbf{va}_j\right| > \pi$. Thus, we wrap $\mathbf{va}_i\widehat{\mathbf{o}_1}\mathbf{va}_j$ to the interval $[-\pi, \pi)$ using the operator $WP(.)$. So, the radius r_1 of C_1 is calculated using geometric relation in a circle as follows:

$$r_1 = \frac{\left\|\mathbf{va}_i - \mathbf{va}_j\right\|}{2 * \sin\left(\left|WP\left(\mathbf{va}_i\widehat{\mathbf{o}_1}\mathbf{va}_j\right)\right|/2\right)} \tag{11}$$

As shown in Figure 3, $\vec{w_1}$ is the perpendicular vector to vector $\mathbf{va}_i\vec{\mathbf{va}}_j$. Hence, knowing the orientation vector of $\mathbf{va}_i\vec{\mathbf{va}}_j$ is equal to $\left(x_{va_i} - x_{va_j}, y_{va_i} - y_{va_j}\right)$, we can define the following perpendicular orientation vector:

$$\vec{w_1} = \left(y_{va_i} - y_{va_j}, -\left(x_{va_i} - x_{va_j}\right)\right) \tag{12}$$

Hence, the coordinates of center $o_1 = (x_{o_1}, y_{o_1})$ for C_1 is defined as follows:

$$x_{o_1} = x_{m_1} \pm \left(\frac{\vec{w_1}(1)}{\left\|\vec{w_1}\right\|}\sqrt{{r_1}^2 - \left(\frac{\left\|\mathbf{va}_i - \mathbf{va}_j\right\|}{2}\right)^2}\right) \tag{13}$$

$$y_{o_1} = y_{m_1} \pm \left(\frac{\vec{w_1}(2)}{\left\|\vec{w_1}\right\|}\sqrt{{r_1}^2 - \left(\frac{\left\|\mathbf{va}_i - \mathbf{va}_j\right\|}{2}\right)^2}\right) \tag{14}$$

where $m_1 = (x_{m_1}, y_{m_1})$ is the midpoint of the chord $(\overline{\mathbf{va}_i\mathbf{va}_j})$. Similarly, we can compute the radius r_2 and the center $o_2 = (x_{o_2}, y_{o_2})$ for the circle C_2. Then, the intersection between C_1 and C_2 is considered as a proper estimation for the receiver position whenever the intersection point is pointed by the orientation vectors $\vec{w_1}$ and $\vec{w_2}$. As well, we choose the solution that validates the angle of arrival for each MPC. As we did for the TL algorithm, we verify if the position estimation is within the room geometry and doesnt belong to any surface in the obstacle set O. This algorithm is repeated over all possible triplets of VANs $(\mathbf{va}_i, \mathbf{va}_j, \mathbf{va}_q), i \neq j \neq q$ that belong to the set VA_{max}. So, we obtain a set of position estimations that represents the intersection between the circumferences C_1 and C_2 determined by the angle differences of arrival δ_1 and δ_2 and the chords $\mathbf{va}_i\vec{\mathbf{va}}_j$ and $\mathbf{va}_j\vec{\mathbf{va}}_k$, $\mathbf{va}_i, \mathbf{va}_j, \mathbf{va}_q \in VA_{max}$. The final estimation of the receiver position is the average of all possible position estimations obtained from the ADoA technique.

III. Context Inference of Room Geometry

After estimating receiver position, our target is to employ context inference for the room via obstacle detection. We introduce obstacle detection in two steps; the first step is estimating the positions of the VANs followed by an estimation of the obstacle direction and obstacle dimensions.

A. Estimation of VANs positions

1) TL for Estimating VANs: We used the TL technique to estimate the position of the receiver assuming we know the location of the VANs in order to solve the system of equations in (2) and (3). Now, our target is to estimate the position of VANs; hence, we proposed to move the receiver to a known position on the same direction of the path from the transmitter to the original receiver position so that we can solve the new system of equations where the unknown variables become the position of the VANs. As known, each ray in the AoA spectrum is either coming from a LOS or a NLOS path. The AoA for any ray may fall in one of the four quadrants in the circle. This aspect has to be taken into consideration while applying the concept of TL algorithm for estimating the VANs positions instead of the receiver one. For instance, assuming that the AoA for the LOS path between the transmitter and receiver and the AoA for the NLOS path (LOS virtually) between the transmitter and receiver (VAN

and receiver) fall in the first quadrant, we develop a system of equation relating the distance between the transmitter and the VAN to be localized using the following systems of equations:

$$\begin{cases} x_{vai_i} - x_{Rx} = \rho_{1,i} \times \cos\theta_{1,i} \\ x_{Rx} - x_{Tx} = \gamma_1 \times \sin\alpha_1 \end{cases} \quad (15)$$

$$\begin{cases} y_{vai_i} - y_{Rx} = \rho_{1,i} \times \sin\theta_{1,i} \\ y_{Rx} - y_{Tx} = \gamma_1 \times \cos\alpha_1 \end{cases} \quad (16)$$

where γ_1 is the distance between the original receiver position and the transmitter, α_1 is the AoA for the LOS link between the transmitter and the receiver, $\rho_{1,i}$ is the distance between the VAN to be localized and the original receiver position and $\theta_{1,i}$ is the AoA for the NLOS link corresponding to $\mathbf{va}_i$. By solving the above two systems of equations, we obtain the following system:

$$\begin{cases} x_{vai_i} - x_{Tx} = \gamma_1 \times \sin\alpha_1 + \rho_{1,i} \times \cos\theta_{1,i} \\ y_{vai_i} - y_{Tx} = \gamma_1 \times \cos\alpha_1 + \rho_{1,i} \times \sin\theta_{1,i} \end{cases} \quad (17)$$

Then we move the receiver to a new position $\mathbf{p}'_{Rx}$ as shown in Figure 4, so that a new AoA spectrum corresponding to the new receiver position is obtained. Similarly, we build a

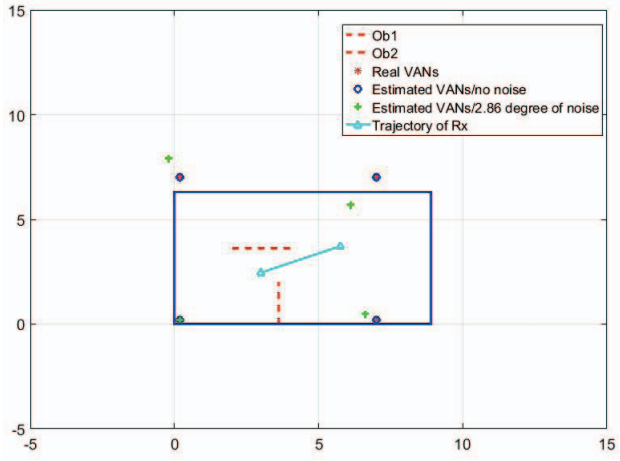

Fig. 4. Estimation VANs by moving the receiver from $\mathbf{p}_{Rx}$ to $\mathbf{p}'_{Rx}$

new system of equation for each AoA entry in the updated AoA spectrum relating the distance between the new receiver position with the transmitter position and the distance between the new receiver position and the VAN to be localized to obtain the following system of equations:

$$\begin{cases} x_{va_i} - x_{Tx} = \gamma_2 \times \sin\alpha_2 + \rho_{2,i} \times \cos\theta_{2,i} \\ y_{va_i} - y_{Tx} = \gamma_2 \times \cos\alpha_2 + \rho_{2,i} \times \sin\theta_{2,i} \end{cases} \quad (18)$$

where $\rho_{2,i}$ is the distance between the VAN to be localized and the new receiver position and $\theta_{2,i}$ is the AoA for the NLOS link corresponding to $\mathbf{va}_i$ and to the update AoA spectrum relative to the new receiver position. We obtain then by solving the systems of equations in (17) and (18) the following system of equation:

$$\begin{cases} \rho_{1,i} \times \cos\theta_{1,i} - \rho_{2,i} \times \cos\theta_{2,i} = \gamma_2 \times \sin\alpha_2 - \gamma_1 \times \sin\alpha_1 \\ \rho_{1,i} \times \sin\theta_{1,i} - \rho_{2,i} \times \sin\theta_{2,i} = \gamma_2 \times \cos\alpha_2 - \gamma_1 \times \cos\alpha_1 \end{cases} \quad (19)$$

Or equivalently:

$$\begin{bmatrix} \cos\theta_{1,i} & -\cos\theta_{2,i} \\ \sin\theta_{1,i} & -\sin\theta_{2,i} \end{bmatrix} \begin{bmatrix} \rho_{1,i} \\ \rho_{2,i} \end{bmatrix} = \begin{bmatrix} -\sin\alpha_1 & \sin\alpha_2 \\ -\cos\alpha_1 & \cos\alpha_2 \end{bmatrix} \begin{bmatrix} \gamma_1 \\ \gamma_2 \end{bmatrix} \quad (20)$$

The two unknowns, $\rho_{1,i}$ and $\rho_{2,i}$, are calculated as follows:

$$\begin{bmatrix} \rho_{1,i} \\ \rho_{2,i} \end{bmatrix} = \Sigma^{-1} \begin{bmatrix} -\sin\alpha_1 & \sin\alpha_2 \\ -\cos\alpha_1 & \cos\alpha_2 \end{bmatrix} \begin{bmatrix} \gamma_1 \\ \gamma_2 \end{bmatrix} \quad (21)$$

where $\Sigma = \begin{bmatrix} \cos\theta_{1,i} & -\cos\theta_{2,i} \\ \sin\theta_{1,i} & -\sin\theta_{2,i} \end{bmatrix}$. Then, we replace $\rho_{1,i}$ and $\rho_{2,i}$ in (17) or (18) to calculate the estimation of x_{va_i} and y_{va_i}. Knowing that MPCs come from the transmitter via a LOS link and from VANs via NLOS links between the transmitter and receiver, we repeat this process over all entries of the AoA power spectrum $SP_{\mathbf{p}}(\theta)$, (a $2 \times N_p$ matrix), to estimate the positions of all VANs.

B. Obstacle Detection

After estimating the VANs, our target is to detect the obstacles in a room. As the VANs are created as mirrors for the transmitter with respect to all surfaces of the obstacles in the room, the obstacles are then the perpendicular to the line connecting the transmitter to each estimated VAN respectively. This perpendicular line passes through the mid-point of the segment $[\mathbf{va}_i\mathbf{p}_{Tx}]$. So, we calculate the slope of this perpendicular segment, where β is the slope of the segment $[\mathbf{va}_i\mathbf{p}_{Tx}]$. Then, we write the equation of the obstacle surface using 1, where $\mathbf{p} = [p_x, p_y]$ becomes the midpoint of segment $[\mathbf{va}_i\mathbf{p}_{Tx}]$. This process is repeated over all pairs of $(\mathbf{va}_i\mathbf{p}_{Tx})$, $i = 1, 2, \ldots, N_{VAN}$, where N_{VAN} is the number of VANs, in order to determine the estimation of all obstacles in the room. Then, we calculate the frequency of each detected obstacle among all pairs $(\mathbf{va}_i\mathbf{p}_{Tx})$. We set an estimation of the surface that has a frequency greater than one, meaning that this obstacle is related to more than one pair of VAN and the transmitter; hence, it will be verified as true obstacle in the room. After detecting the direction of the obstacles in the

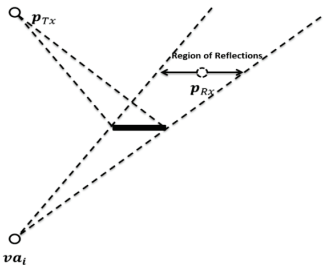

Fig. 5. Region of possible reflections

room, we are left with setting the dimensions of the obstacle. As shown in Figure 5, the receiver can move within the region of all possible reflections determined by a horizontal limited obstacle, the position of the transmitter, and the related VAN. Hence, the AoA spectrum generated at all receiver positions will decay when the receiver leaves the region of reflections. So, for instance, and without loss of generality, for a horizontal obstacle, we will move the receiver in small steps to the right and to the left, parallel to the obstacle direction, and we keep on checking the amplitude in the AoA spectrum corresponding to the VAN that is responsible of obstacle reflections with respect to the transmitter. When the amplitude decays significantly, it means that the receiver left the beam of all possible reflections corresponding to the obstacle and the related VAN. Hence, we know that we reached the right and the left limit of the obstacle. We remind the reader that

the direction of the obstacle is easily detected through the perpendicular between the transmitter and the VANs.

IV. Simulation Results

The room geometry is of rectangular type of size 8.9×6.3 m. We take the south-western corner of the room to be the reference of the Cartesian coordinate system. The angles are measured with respect to the positive part of the x-axis. The transmitter is set at position $\mathbf{p}_{Tx} = (0.2, 0.2)$ m. We assume the antenna at the transmitter to be omnidirectional; hence, the transmitted power $P_{Tx}(\theta)$ is constant for all θ. Instead, antenna array is used at the receiver with a reception beam pattern described as $P_{Rx}(\theta) = \exp\left(-\frac{\theta^2}{2s^2}\right)$, $s = 0.1$. The value of parameter s and the Gaussian shape have been devised empirically. Additionally, all results were implemented for 10000 realizations. The CDF for the localization error shown

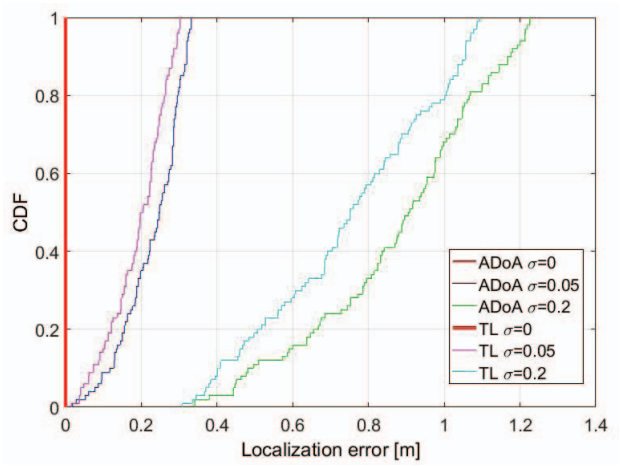

Fig. 6. Localization error CDF for TL and ADoA for different values of $\sigma\,(rad)$

in Figure 6 shows that for ideal case, where $\sigma = 0°$, both the TL and the ADoA techniques localize the receiver with full accuracy. When the value of σ increases, the accuracy of localization achieved using TL and ADOA decreases. For instance, when $\sigma = 0.05rad = 2.86°$, the accuracy of localization achieved with TL and ADoA is almost 0.3 m. Additional increase in the noise to reach $\sigma = 0.2rad = 11.45°$, localization accuracy decreases to reach an error of more than 1 m at 90% of the estimates. Moreover, we can observe from Figure 6 that TL achieves higher localization accuracy compared to ADoA as we increase σ. As well, we simulated the performance of the proposed localization technique for estimating the VANs followed by obstacle detection. First, we test the TL technique for estimating the VANs. Figure 7 shows the CDF of the RMSE for localizing the VANs using the TL algorithm. As deduced from the CDF of the estimation error for localizing the receiver, as $\sigma_{radians}$ increases from 0° to 11.45°, the error will increase from 0 m to reach almost 5 m.

A. Obstacle Estimation

We estimate the obstacles in the room with their limits. The simulated scenario shows that the horizontal and vertical obstacles are properly detected as shown in Figure 8. Nevertheless, the limits of the detected obstacles are estimated with certain error shown in Figure 9. The results show an increase in the error of estimating obstacle limits with the increase in the noise standard deviations.

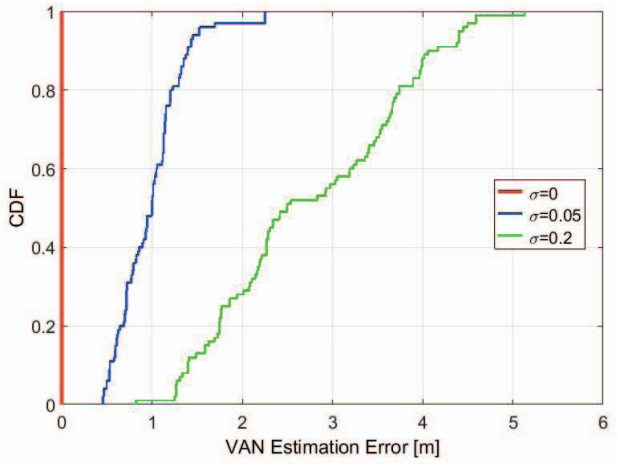

Fig. 7. CDF for Estimation Error of VANs using TL

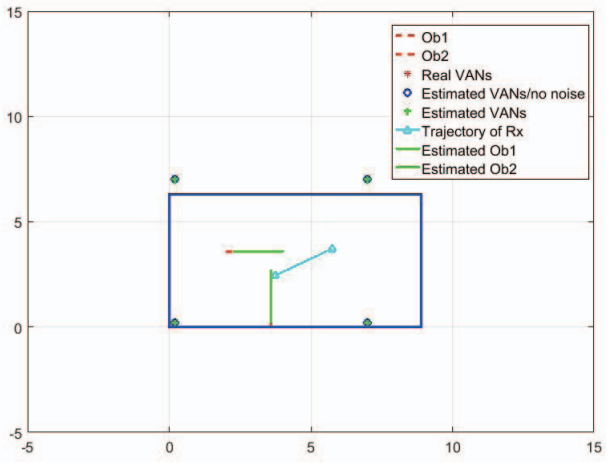

Fig. 8. Estimation of Room Geometry using TL for horizontal and vertical obstacles

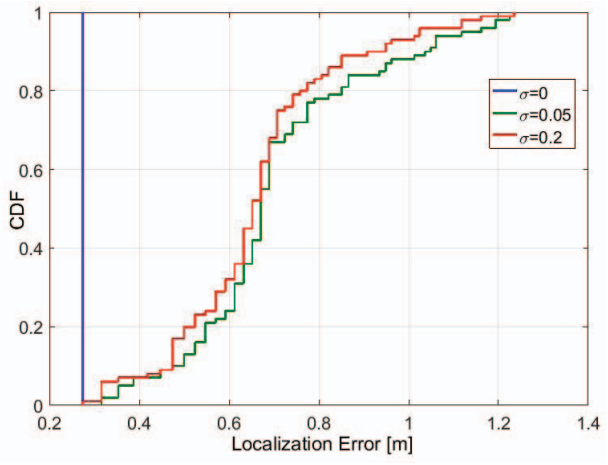

Fig. 9. CDF for Estimation Error of Obstacle Limits using TL

V. Conclusion

We presented in this paper the localization of a single receiver in an indoor scenario of single AP with MMW propagation characteristics using TL and ADoA techniques. The performance of the techniques is tested through simulations in terms of CDF of the location estimation error. As well, we proposed context inference of the room via obstacle detection. This approach is based on estimating first the VANs assuming that we know the position of the receiver. Then, horizontal and vertical obstacles are detected and their limits are estimated using the concept of mirroring. Here, high accuracy has been obtained. In the future, we will investigate the localization of moving objects and the specification of these objects through reflection indices.

References

[1] T. Rappaport et al., *Millimeter Wave Wireless Communications*. Pearson Education, 2014.

[2] S. Rangan, T. Rappaport, and E. Erkip, "Millimeter-wave cellular wireless networks: Potentials and challenges", *Proceedings of the IEEE*, vol. 102, no. 3, pp. 366385, Mar. 2014. J.

[3] Thompson et al., "5G wireless communication systems: prospects and challenges", *IEEE Commun. Mag.*, vol. 52, no. 2, pp. 6264, Feb. 2014.

[4] T. Rappaport et al., "Millimeter wave mobile communications for 5G cellular: It will work!" *IEEE Access*, vol. 1, pp. 335349, 2013.

[5] A. Kupper. Location-based services. Wiley, 2005

[6] E. Torkildson, H. Zhang, and U. Madhow, "Channel modeling for millimeter wave MIMO", in *Proc. Information Theory and Applications Workshop*, San Diego, CA, Jan. 2010.

[7] M. K. Samimi and T. S. Rappaport, "Statistical Channel Model with Multi-Frequency and Arbitrary Antenna Beamwidth for Millimeter-Wave Outdoor Communications", *2015 IEEE Globecom Workshops (GC Wkshps)*, San Diego, CA, 2015, pp. 1-7.

[8] L. Subrt, P. Pechac, and S. Zvanovec, "New approach to modeling of diffuse reflection and scattering for millimeter-wave systems in indoor scenarios", *PIERS Online*, vol. 6, 2010.

[9] N. Peinecke, H. Doehler, and B. Korn, "Phong-like lighting for MMW radar simulation", *in Proc. SPIE*, Cardiff, UK, 2008.

[10] A. Maltsev et al., "Experimental investigations of 60 GHz WLAN systems in office environment", *IEEE J. Sel. Areas Commun.*, vol. 27, no. 8, pp. 14881499, Oct. 2009.

[11] G. R. MacCartney et al., "Path loss models for 5G millimeter wave propagation channels in urban microcells", *in Proc. IEEE GLOBECOM*, Atlanta, GA, Dec. 2013.

[12] T. Rappaport et al., "Broadband millimeter-wave propagation measurements and models using adaptive-beam antennas for outdoor urban cellular communications", *IEEE Trans. Antennas Propag.*, vol. 61, no. 4, pp. 18501859, Apr. 2013.

[13] M. Bocquet, N. Obeid, C. Loyez, C. Lethien, F. Boukour, N. Rolland, and M. Heddebaut, "Comparison between 60-GHz UWB frequency modulation and UWB impulse-radio location systems", *in Radar Conference*,2008. EuRAD 2008. European, Oct. 2008, pp. 4143.

[14] H. R. Fang, G. P. Cao, E. A. Gharavol, K. Tom, and K. Mouthaan, "60 GHz short range planar RSS localization", *in Proceedings of Asia-Pacific Microwave Conference 2010*, 2010.

[15] A. Jafari, J. Sarrazin, D. Lautru, A. Benlarbi-Dela, L. Petrillo and P. De Doncker, "NLOS influence on 60 GHz indoor localization based on a new TDOA extraction approach," *2013 European Microwave Conference*, Nuremberg, 2013, pp. 330-333.

[16] D. Dardari, A. Conti, U. Ferner, A. Giorgetti, and M. Z. Win, Ranging With Ultrawide Bandwidth Signals in Multipath Environments, *Proceedings of the IEEE*, vol. 97, no. 2, pp. 404426, Feb. 2009.

[17] A. Conti, M. Guerra, D. Dardari, N. Decarli, and M. Z. Win, Network Experimentation for Cooperative Localization, *IEEE JOURNAL ON SELECTED AREAS IN COMMUNICATIONS*, vol. 30, no. 2, Feb. 2012.

[18] A. Olivier, G. Bielsa, I. Tejado, M. Zorzi, J. Widmer and P. Casari, "Lightweight Indoor Localization for 60-GHz Millimeter Wave Systems," *2016 13th Annual IEEE International Conference on Sensing, Communication, and Networking (SECON)*, London, 2016, pp. 1-9.

[19] T. Kos, M. Grgic, and G. Sisul, "Mobile user positioning in gsm/umts cellular networks", *in Multimedia Signal Processing and Communications*, 48th International Symposium ELMAR-2006 focused on, Zadar, Croatia, Jun. 2006.

[20] P. Meissner, T. Gigl, and K. Witrisal, "UWB sequential monte carlo positioning using virtual anchors," *in Proc. IPIN*, Zurich, Switzerland, Sep. 2010.